Atmos. Meas. Tech., 11, 3339–3350, 2018
https://doi.org/10.5194/amt-11-3339-2018
© Author(s) 2018. This work is distributed under
the Creative Commons Attribution 4.0 License.

Atmospheric Measurement Techniques
Open Access
EGU

A full-mission data set of H_2O and HDO columns from SCIAMACHY 2.3 µm reflectance measurements

Andreas Schneider, Tobias Borsdorff, Joost aan de Brugh, Haili Hu, and Jochen Landgraf

Earth science group, SRON Netherlands Institute for Space Research, Utrecht, the Netherlands

Correspondence: Andreas Schneider (a.schneider@sron.nl)

Received: 30 December 2017 – Discussion started: 2 March 2018
Revised: 4 May 2018 – Accepted: 24 May 2018 – Published: 12 June 2018

Abstract. A new data set of vertical column densities of the water vapour isotopologues H_2O and HDO from the SCanning Imaging Absorption spectroMeter for Atmospheric CHartographY (SCIAMACHY) instrument for the whole of the mission period from January 2003 to April 2012 is presented. The data are retrieved from reflectance measurements in the spectral range 2339 to 2383 nm with the Shortwave Infrared CO Retrieval (SICOR) algorithm, ignoring atmospheric light scattering in the measurement simulation. The retrievals are validated with ground-based Fourier transform infrared measurements obtained within the Multi-platform remote Sensing of Isotopologues for investigating the Cycle of Atmospheric water (MUSICA) project. A good agreement for low-altitude stations is found with an average bias of -3.6×10^{21} for H_2O and -1.0×10^{18} molec cm^{-2} for HDO. The a posteriori computed δD shows an average bias of -8 ‰, even though polar stations have a larger negative bias. The latter is due to the large amount of sensor noise in SCIAMACHY in combination with low albedo and high solar zenith angles. To demonstrate the benefit of accounting for light scattering in the retrieval, the quality of the data product fitting effective cloud parameters simultaneously with trace gas columns is evaluated in a dedicated case study for measurements round high-altitude stations. Due to a large altitude difference between the satellite ground pixel and the mountain station, clear-sky scenes yield a large bias, resulting in a δD bias of 125 ‰. When selecting scenes with optically thick clouds within 1000 m above or below the station altitude, the bias in a posteriori δD is reduced from 125 to 44 ‰. The insights from the present study will also benefit the analysis of the data from the new Sentinel-5 Precursor mission.

1 Introduction

Atmospheric water vapour is a trace gas which is important for the energy budget of the atmosphere. For instance, it is the strongest natural greenhouse gas and transports energy through latent heat (e.g. Kiehl and Trenberth, 1997; Harries, 1997). However, the uncertainties regarding the effects of water vapour in the energy balance of the atmosphere and regarding the interaction between water vapour and the atmospheric circulation are still large (e.g. Stevens and Bony, 2013). Measurements are expected to contribute to a better understanding and quantification of these processes. Observations of isotopologues of water are especially interesting, because the ratio provides information about the history of the sampled air parcel due to a temperature-dependent isotopic fractionation during evaporation and condensation caused by different vapour pressure and diffusion constants of the isotopologues (e.g. Dansgaard, 1964). For instance, when water is evaporated from a reservoir that is not too small, heavy isotopologues are depleted. Water vapour is also depleted by condensation during the formation of clouds and precipitation. In all these cases the amount of depletion depends on temperature.

The ratio of the isotopologues HDO and H_2O for column densities c_{HDO} and $c_{\mathrm{H_2O}}$ is defined by $R_\mathrm{D} = c_{\mathrm{HDO}}/c_{\mathrm{H_2O}}$. The depletion is usually described by the relative difference between an observed ratio R_D and a standard ratio $R_{\mathrm{D,std}}$:

$$\delta\mathrm{D} = \frac{R_\mathrm{D} - R_{\mathrm{D,std}}}{R_{\mathrm{D,std}}} \cdot 1000\,‰\,. \quad (1)$$

This is a column δD, which some authors refer to as $\overline{\delta\mathrm{D}}$ to distinguish it from δD profiles. The commonly used standard ratio is Vienna Standard Mean Ocean Water (VSMOW), $R_{\mathrm{D,std}} = 3.1152 \times 10^{-4}$.

Published by Copernicus Publications on behalf of the European Geosciences Union.

Measurements of atmospheric water vapour isotopologues are rare. Observations are made in situ with aircraft and balloons (e.g. Rinsland et al., 1984; Stowasser et al., 1999; Ehhalt et al., 2005; Dyroff et al., 2010), in situ on the ground (e.g. Wen et al., 2010; Bastrikov et al., 2014) and by using (ground- or space-based) remote sensing techniques. Ground-based remote sensing of the water vapour isotopologues is usually carried out using Fourier transform infrared (FTIR) instruments, which observe the direct sunlight in the infrared, determining the vertically integrated columns above the site. Many ground stations are organised in networks, such as the Total Carbon Column Observing Network (TCCON, https://tccondata.org/, last access: 6 June 2018) and the Network for the Detection of Atmospheric Composition Change (NDACC, www.ndacc.org, last access: 6 June 2018). Within the latter, the Multi-platform remote Sensing of Isotopologues for investigating the Cycle of Atmospheric water (MUSICA) project (Schneider et al., 2016) provides a validation against in situ measurements. Satellite-based measurements have the advantage of global coverage. H_2O and HDO were first retrieved from satellite data by Zakharov et al. (2004) using thermal infrared measurements from the Interferometric Monitor for Greenhouse gases (IMG) sensor aboard the Advanced Earth Observing Satellite (ADEOS). Later, these isotopologues were also inferred from the Tropospheric Emission Spectrometer (TES) on the Earth Observing System (EOS) Aura satellite (Worden et al., 2006), the Michelson Interferometer for Passive Atmospheric Sounding (MIPAS) aboard European Space Agency (ESA)'s environmental satellite (ENVISAT) (Steinwagner et al., 2007), the Infrared Atmospheric Sounding Interferometer (IASI) aboard the MetOP satellite (Herbin et al., 2009) and the Greenhouse Gases Observing Satellite (GOSAT) (Boesch et al., 2013). Frankenberg et al. (2009) used the short-wave infrared (SWIR) band of the SCanning Imaging Absorption spectroMeter for Atmospheric CHartographY (SCIAMACHY) instrument (Bovensmann et al., 1999) on ENVISAT to obtain 3 years of simultaneous measurements of H_2O and HDO. This data set was extended to the period 2003–2007 by Scheepmaker et al. (2015). In the present study a new H_2O and HDO data set for the whole of the mission period of SCIAMACHY is presented.

Recently, the new Tropospheric Monitoring Instrument (TROPOMI) aboard the Sentinel-5 Precursor satellite (Veefkind et al., 2012) was launched, which includes the SWIR in the same spectral range and with the same spectral resolution as SCIAMACHY, but at much better signal-to-noise ratio (SNR) and spatial resolution. It is expected that retrievals from this new instrument will provide H_2O and HDO data of unprecedented quality. The present study is also preparation for the new mission, apart from providing a data set for the whole of the mission period of SCIAMACHY.

The new data set is retrieved using the Shortwave Infrared CO Retrieval (SICOR) algorithm as discussed by Scheepmaker et al. (2016); Landgraf et al. (2016); Borsdorff et al. (2016, 2017). SICOR is designed for the operational processing of carbon monoxide total column retrieval from TROPOMI measurements. The algorithm has two options. First, assuming a strict cloud filtering, the retrieval ignores atmospheric scattering in the SWIR spectral range, and the atmospheric total column of CH_4, H_2O, HDO and CO is inferred from the measurement. This approach, called non-scattering retrieval in this paper, is proposed by Scheepmaker et al. (2016) to generate the TROPOMI H_2O and HDO data product. In this study, the retrieval is applied to SCIAMACHY observations, and the H_2O and HDO data product is validated against ground-based measurements from MUSICA. Alternatively, one can choose a loose cloud clearing. Here, the optical depth and height of a scattering layer is retrieved from the CH_4 absorptions of the measurement using appropriate a priori information from chemical transport models (CTMs). This approach, hereinafter referred to as scattering retrieval, is the processing baseline for CO retrievals from SCIAMACHY and TROPOMI as discussed by Landgraf et al. (2016); Borsdorff et al. (2017). In the present paper, this approach is evaluated for the retrieval of water vapour isotopologues by comparing ground-based observations at high-altitudes with collocated SCIAMACHY retrievals using observations with clouds at a height similar to that of the ground site.

The remainder of this article is structured as follows: in Sect. 2 the retrieval set-ups of both the non-scattering and scattering retrieval are given. Section 3 presents the validation of the non-scattering data product, whereas Sect. 4 discusses the potential added value of the scattering retrieval of the water isotopologues. Finally, a summary is given and conclusions are drawn in Sect. 5.

2 Retrieval method

The SICOR algorithm and its application to CO and HDO/H_2O retrievals is discussed in detail by Scheepmaker et al. (2016); Landgraf et al. (2016); Borsdorff et al. (2016, 2017). In this section its main features that are relevant in the context of this study are summarised.

SICOR provides two options for the trace gas column retrieval from SWIR radiance measurements. First, assuming clear-sky observations, atmospheric scattering is ignored in the forward simulation of the measurement. Subsequently the algorithm infers the total column of H_2O, HDO, CH_4 and CO together with the Lambertian surface albedo from SCIAMACHY's channel 8 measurements between 2338.5 and 2382.5 nm. This spectral fit window is an extension of the one proposed by Scheepmaker et al. (2015) and includes more absorption lines of HDO, which is beneficial for retrievals using measurements at the end of SCIAMACHY's lifespan (which was not considered by Scheepmaker et al., 2015), when more and more pixels ceased to function. Spectral absorption line data are taken from Scheepmaker et al.

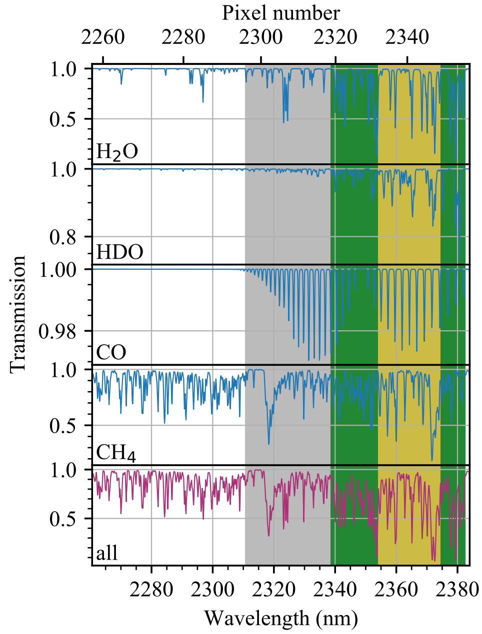

Figure 1. Simulation of atmospheric absorption in the spectral range of SCIAMACHY's channel 8 for the absorbers taken into account by the retrieval algorithm. The grey shading marks the retrieval window for CO used by Borsdorff et al. (2016, 2017), the yellow shading marks the window for H_2O and HDO used by Scheepmaker et al. (2015) and the green shading marks the extension of that window used in this work.

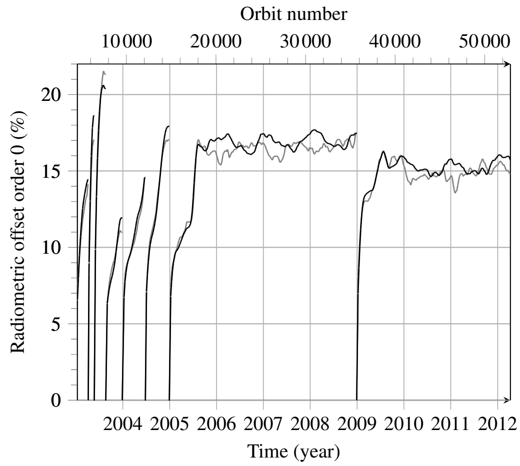

Figure 2. Zero-order radiometric offset retrieved from cloud-free SCIAMACHY spectra above the Sahara (black) and Australia (grey). The additive offset is given as a percentage of the total radiance.

(2013); Rothman et al. (2009); Predoi-Cross et al. (2006). The atmospheric absorption within this spectral range is presented in Fig. 1. The trace gas column retrieval utilises the profile-scaling approach as described in detail by Borsdorff et al. (2014). The a priori profiles of water vapour are adapted from the European Centre for Medium-Range Weather Forecasts (ECMWF) reanalysis product. Since the ECMWF data product does not provide the individual isotopologue profiles, H_2O and HDO profiles are obtained from the water vapour profile by scaling it with the standard abundances of H_2O and HDO. A priori profiles for methane and CO are taken from TM5 simulations. Obviously, the assumption of clear-sky observations requires cloud clearing of the data, which is performed a posteriori to the retrieval. As proposed by Scheepmaker et al. (2015), only retrieved data which satisfy the following conditions are considered:

$$0.9 < \frac{c_{CH_4}}{c_{CH_4,TM5}} < 1.1 \tag{2}$$

$$0.7 < \frac{c_{H_2O}}{c_{H_2O,ECMWF}}, \tag{3}$$

with the retrieved columns c_{CH_4} and c_{H_2O} and the corresponding model predictions $c_{CH_4,TM5}$ and $c_{H_2O,ECMWF}$. Moreover, due to radiometric performance issues with SCIAMACHY in the SWIR spectral range, the data have to be filtered with respect to outliers. Since water vapour in the troposphere is log-normally distributed (Schneider et al., 2006) and (as seen in our data) so is its uncertainty, the 15.9th and 84.1th percentiles $P_{15.9}$ and $P_{84.1}$ of the logarithmic H_2O and HDO uncertainty data distributions $\log e$ are considered to define

$$\sigma = \frac{1}{2}(P_{84.1} - P_{15.9}) \,. \tag{4}$$

Only data within 5σ around the median μ of the logarithmic distribution are used. A similar filter is applied to the root mean square of the spectral fit residual, c_{rms}, where data points within 6σ around the median μ are kept. Thus,

$$\mu_{e(H_2O)} - 5\sigma_{e(H_2O)} < \log e_{H_2O} < \mu_{e(H_2O)} + 5\sigma_{e(H_2O)} \tag{5}$$

$$\mu_{e(HDO)} - 5\sigma_{e(HDO)} < \log e_{HDO} < \mu_{e(HDO)} + 5\sigma_{e(HDO)} \tag{6}$$

$$\mu_{rms} - 6\sigma_{rms} < \log c_{rms} < \mu_{rms} + 6\sigma_{rms}. \tag{7}$$

Furthermore, the data are screened with respect to the number of iterations, $N_{iter} \leq 12$, and the solar zenith angle (SZA), $\vartheta_{sz} < 70°$.

Alternatively, SICOR allows atmospheric scattering in the retrieval to be accounted for and so enhances the data yield of the retrieval. Based on the numerically very efficient two-stream radiative transfer model (Landgraf et al., 2016), the retrieval uses prior model information on CH_4 to infer the height h_{cld} and optical depth τ_{cld} of a scattering layer together with the total column of CO, H_2O and HDO and the Lambertian surface albedo. Using this approach, our study considers, for the first time, the retrieval of the water vapour isotopologues in the SWIR for cloudy atmospheres and demonstrates the added value of the approach for the data product. The same quality filter as described above is used. The cloud filtering is detailed in Sect. 4.

The performance of SCIAMACHY suffered from an ice layer build-up on the SWIR detector (e.g. Gloudemans et al., 2005). Among other things, this caused additional stray light in the instrument, meaning in a first approximation an additive radiometric bias to the measurement. To compensate for this effect, a radiometric correction as described by Borsdorff et al. (2016) is applied. Hence, a radiometric offset with spectral dependence described by a third-order polynomial is fitted for clear-sky scenes above the Sahara region with a high albedo and so a high SNR while fixing methane to the prior TM5 model information. Using the fitting window 2338.5–2382.5 nm, the time series of the spectrally constant radiometric offset is plotted in Fig. 2. It shows an increasing offset with a growing ice layer which resets to zero at so-called decontamination events during which the detector was heated to remove the ice. Since 2005 no regular decontamination procedures have been carried out except for one additional decontamination at the beginning of 2009. Due to that the offset eventually stabilised. To demonstrate that the calibration is globally applicable, the figure also shows the offset determined above Australia. The results are very similar and the deviation between the radiometric biases is less than 10 % when disregarding three outliers in the vicinity of decontamination events and a short period at the beginning of 2011 with a deviation of ∼14 %.

The strategy for the data product presented in this paper is to provide H_2O and HDO columns for the whole period of the SCIAMACHY mission. The ratio δD may be computed a posteriori from these data but is not a primary product.

3 Validation of the non-scattering retrieval of H_2O and HDO

To validate the SCIAMACHY H_2O and HDO total columns, the observations are compared to ground-based FTIR measurements from nine NDACC-MUSICA stations (Barthlott et al., 2017; Schneider et al., 2016, 2012), which are listed in Table 1. Here, high-altitude stations like Jungfraujoch (3580 m a.s.l.) and Izaña (2367 m a.s.l.) are not considered because the satellite and ground-based measurements probe different altitude ranges for these cases.

For each site, all SCIAMACHY observations are selected that pass the filter described in Sect. 2 and are within a radius of 800 km around the station. Finally for comparison, both for MUSICA and SCIAMACHY data, monthly medians are taken, so that the data with different sampling can be compared. Months in which the number of individual measurements contributing to the median is less than 5 % of that in the month with most data are excluded to avoid biases by bad statistics. The loose spatio-temporal coregistration criteria are required to include a sufficient number of measurements to overcome the large amount of measurement noise in SCIAMACHY. Even though water vapour may change substantially over small distances, the results suggest that representation errors due to the large spatial collocation area average out in the monthly medians and their statistics.

Table 1. List of MUSICA ground stations used for the validation.

Station name	Latitude	Longitude	Altitude	Time period
Eureka	80.1° N	86.4° W	610 m	2006–2014
Ny Ålesund	78.9° N	11.9° E	21 m	2005–2014
Kiruna	67.8° N	20.4° E	419 m	1996–2014
Bremen	53.1° N	8.9° E	27 m	2004–2014
Karlsruhe	49.1° N	8.4° E	110 m	2010–2014
Jungfraujoch	46.6° N	8.0° E	3580 m	1996–2014
Izaña	28.3° N	16.5° W	2367 m	1999–2014
Wollongong	34.5° S	150.9° E	30 m	2007–2014
Lauder	45.1° S	169.7° E	370 m	1997–2014

Figure 3 depicts a time series of monthly medians for the station Bremen. For all three quantities H_2O, HDO and δD, the measurements of both instruments agree well. The biases, which are defined as the average of the difference between SCIAMACHY and MUSICA results, are -5.6×10^{20} molec cm^{-2}, -1.4×10^{17} molec cm^{-2} and $+11$ ‰. The conversion factor to precipitable water in mm is 2.99×10^{-22} for H_2O and 3.16×10^{-22} mm molec^{-1} cm^2 for HDO. The time series also shows that the data set is homogeneous throughout the whole mission period. Figure 4 shows a clear correlation between MUSICA and SCIAMACHY measurements for all three quantities with Pearson correlation coefficients of 0.81, 0.81 and 0.63 for H_2O, HDO and δD.

The statistics for all low-altitude MUSICA stations are presented in Fig. 5. For H_2O and HDO, the correlation is good (between 0.74 and 0.97), with small biases for all stations (on average -3.6×10^{21} and -1.0×10^{18} molec cm^{-2}). Also, for δD, a good correlation between SCIAMACHY and MUSICA data is achieved for most stations, but it is only mediocre for Kiruna, Wollongong and Lauder. The reason is that the seasonality in δD is weak for those stations. To demonstrate that the low correlation coefficient does not indicate bad results, the time series for Lauder (for which the correlation is lowest) is shown in Fig. 6. The polar stations Eureka and Ny Ålesund have a relatively high bias in δD. Although the number of observations is large due to orbits converging at polar latitudes, the results are dominated by difficult measurement conditions with low surface albedos and high solar zenith angles in combination with SCIAMACHY's high amount of sensor noise, making them imprecise. The average bias in δD over all stations is -8 ‰.

The bias is relatively stable over the mission time. When computing the bias for both halves of the mission from 2003 to 2007 and from 2008 to 2012, the difference is relatively small for most stations. On average the relative difference in bias in H_2O between the halves is 20 %, with a larger difference for Bremen, where it changes from -2.9×10^{21} to -8.2×10^{21} molec cm^{-2}. On the other hand, the bias in δD does not change in Bremen. The mean change in the bias

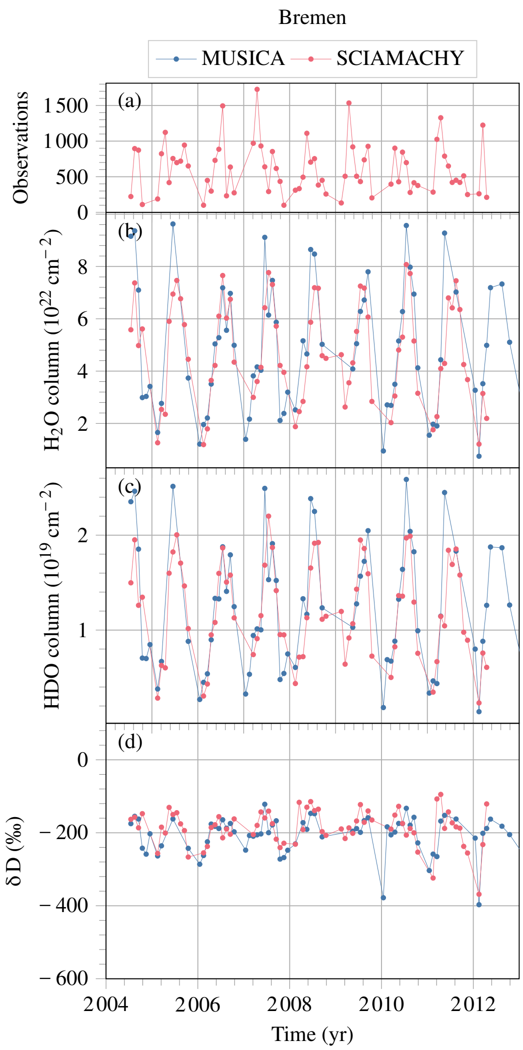

Figure 3. Time series of monthly medians of H_2O **(b)**, HDO **(c)** and δD **(d)** for the MUSICA ground station Bremen (blue) and collocated SCIAMACHY observations for clear-sky conditions (red). Panel **(a)** shows the number of SCIAMACHY measurements in each month.

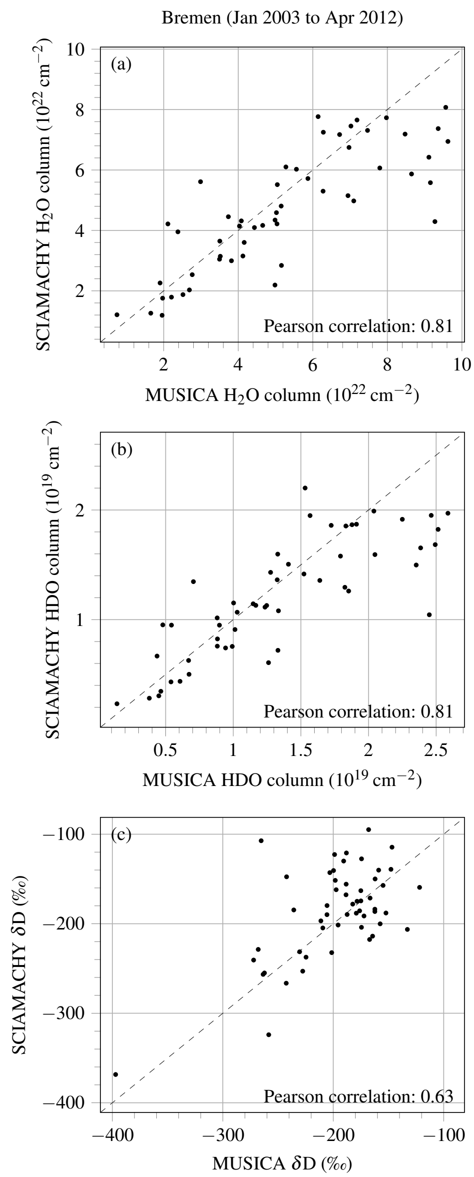

Figure 4. Correlation plots for monthly medians of MUSICA and SCIAMACHY observations of H_2O **(a)**, HDO **(b)** and δD **(c)** at the station Bremen between January 2003 and April 2012.

of δD is 11 %. Only for Ny Ålesund does the bias in δD become significantly worse from −24 ‰ for 2003–2007 to −52 ‰ for 2008–2012. The latter is attributed to the degradation of the instrument, which especially plays a role for difficult measurement conditions as described above. Low sun and low albedo result in low SNR and thus higher error sensitivity. Outside polar latitudes easier measurement conditions can make up for the degradation.

To demonstrate the coverage of the non-scattering retrieval data set, world plots of H_2O, HDO and δD averaged over the first and second half of the mission period are presented in the left and right panels of Fig. 7. In H_2O and HDO the latitudinal gradient with more water vapour abundance in the tropics and drier air in polar regions is clearly visible. Above mountain ranges such as the Andes and the Himalayas, the water vapour abundance is reduced. This effect is discussed in more detail in the next section in connection with high-altitude stations. A continental effect with drier air inland can also be seen, e.g. in North America, North Africa and Asia. In δD, the features described by Scheepmaker et al. (2015) and Frankenberg et al. (2009) are mostly reproduced. On a large scale, δD decreases from the equator to the poles, which has already been mentioned by Dansgaard (1964). High altitudes also show strong depletion in δD. The continental effect is visible, for example, in North and South America, Asia and even Australia. Enhanced δD above the Red Sea

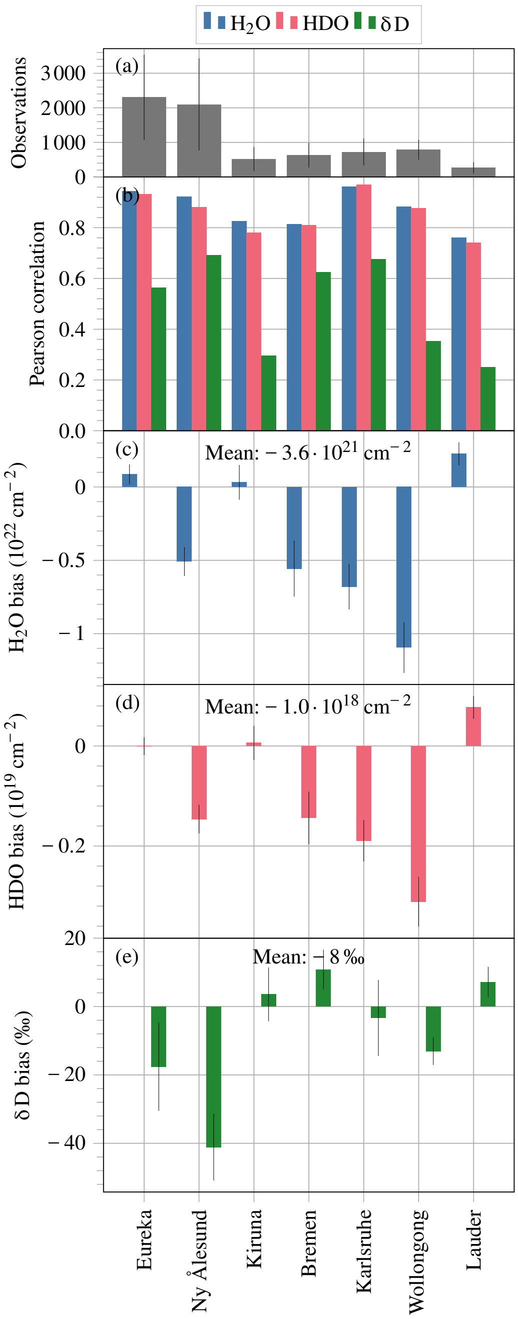

Figure 5. Statistics for the validation of the non-scattering retrievals: **(a)** average number of measurements per month and their standard deviation. **(b)** Pearson correlation coefficient between MUSICA and SCIAMACHY monthly averages of H_2O (blue), HDO (red) and δD (green). **(c)** Bias of H_2O and its standard error. **(d)** Bias of HDO and its standard error. **(e)** Bias of δD and its standard error.

seen by Frankenberg et al. (2009) is also reproduced. More importantly, the comparison between the left and right panels shows that the data set is consistent throughout the mission time.

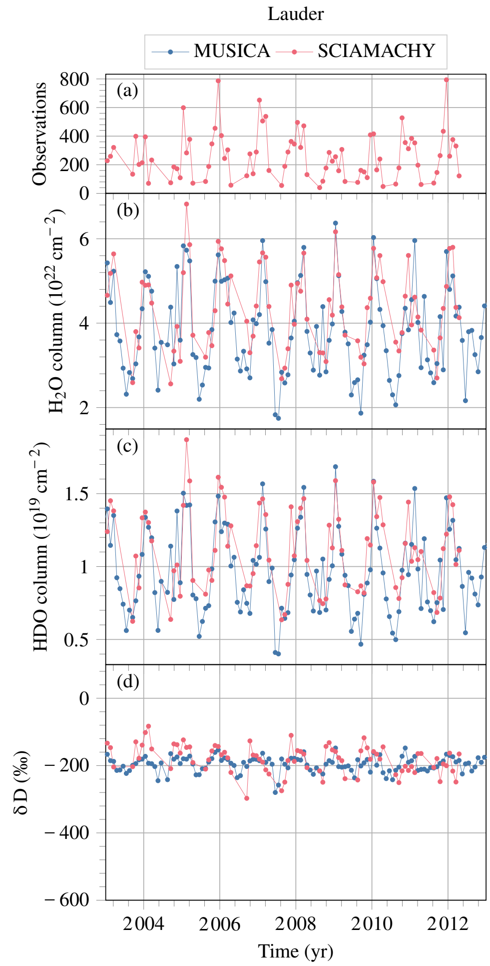

Figure 6. Same as Fig. 3, but for the station Lauder.

4 The scattering retrieval of H_2O and HDO

To demonstrate the benefit of accounting for light scattering by clouds in the retrieval of H_2O and HDO, the corresponding water vapour isotopologue product of SCIAMACHY is compared with MUSICA measurements at elevated sites above 2000 m a.s.l. Here, significant differences between the mean surface height of the SCIAMACHY ground pixels and the surface elevation of the ground site hampers the verification of the measurements using clear-sky observations. However, when retrieving cloud height and scattering optical depth jointly with the water columns, satellite and ground-based measurements of similar altitude sensitivity can be selected. This is demonstrated for the MUSICA site at Jungfraujoch (3580 m a.s.l.) by selecting collocated SCIAMACHY observations for clear-sky and cloudy-sky conditions using the selection criteria in Table 2.

A time series of clear-sky observations in the left panel of Fig. 8 shows large biases in the SCIAMACHY measurements relative to MUSICA of 4.3×10^{22} molec cm^{-2} in H_2O,

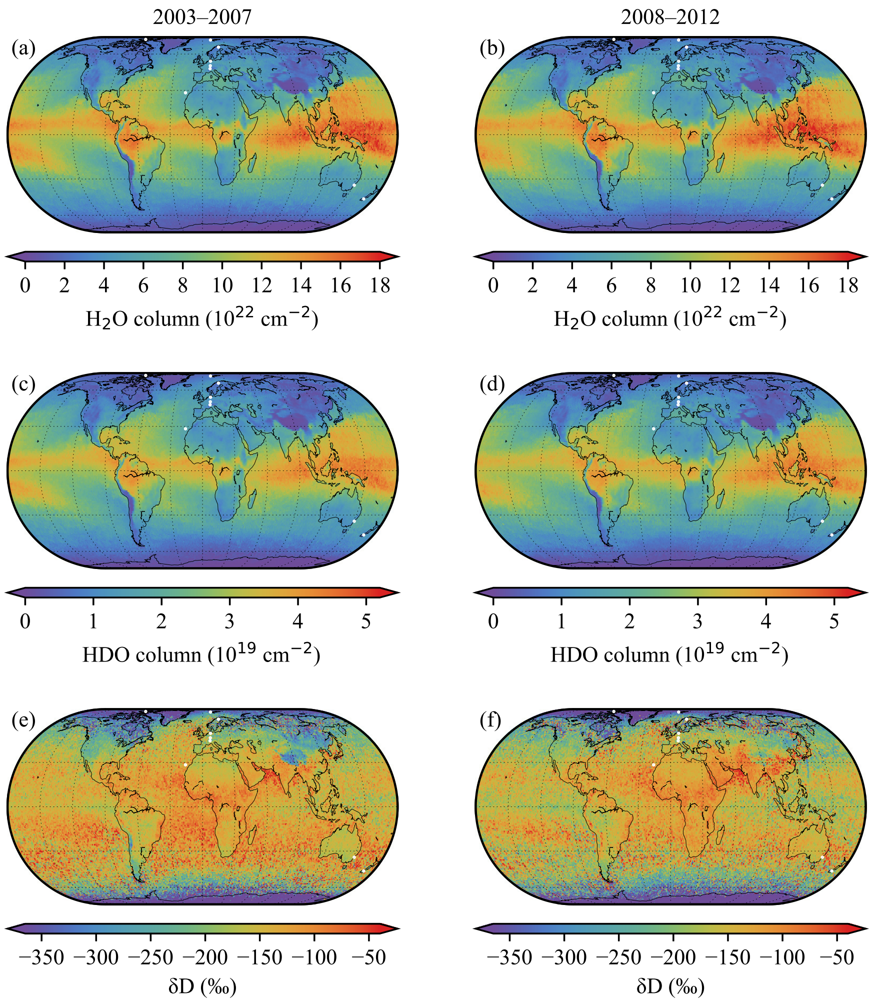

Figure 7. H_2O column **(a, b)**, HDO column **(c, d)** and δD **(e, f)** on a $1^\circ \times 1^\circ$grid averaged over the first half from 2003 to 2007 (left) and the second half from 2008 to 2012 (right) of the SCIAMACHY mission. The white points mark the locations of the MUSICA stations used for validation.

Table 2. Selection criteria for clear-sky and cloudy-sky conditions using scattering retrieval. Here h_s is the altitude of the MUSICA ground site and max(SNR) is the maximum of the signal-to-noise ratio of a spectrum.

Quantity	Filter
Clear-sky filter	
Cloud height	$h_{cld} < 1000$ m
Cloud optical thickness	$\tau_{cld} < 0.2$
SNR	$5 \leq \max(\mathrm{SNR}) \leq 150$
Filter for optically thick clouds	
Cloud height	$h_s - 1000\,\mathrm{m} \leq h_{cld} \leq h_s + 1000\,\mathrm{m}$
Cloud optical thickness	$\tau_{cld} > 3$

1.1×10^{19} molec cm^{-2} in HDO and 140 ‰ in δD. Atop the mountain at Jungfraujoch, only the partial column above 3580 m is observed, while SCIAMACHY in a collocation radius of 800 km around the site observes the whole column above the ground pixel, which has a much lower elevation than Jungfraujoch for most scenes. With the large vertical gradient of water vapour abundance in the lower troposphere, this leads to the observed bias. Moreover, the column-averaged δD has lower values over mountains due to the HDO depletion with height.

To correct the SCIAMACHY observations for this altitude difference, the collocated ECMWF water vapour profile is scaled to the total column observed by SCIAMACHY, and subsequently the scaled profile is truncated at the height of Jungfraujoch. The vertical integration of this truncated profile provides the altitude-corrected H_2O and HDO columns depicted in the centre panels of Fig. 8. Obviously, the cor-

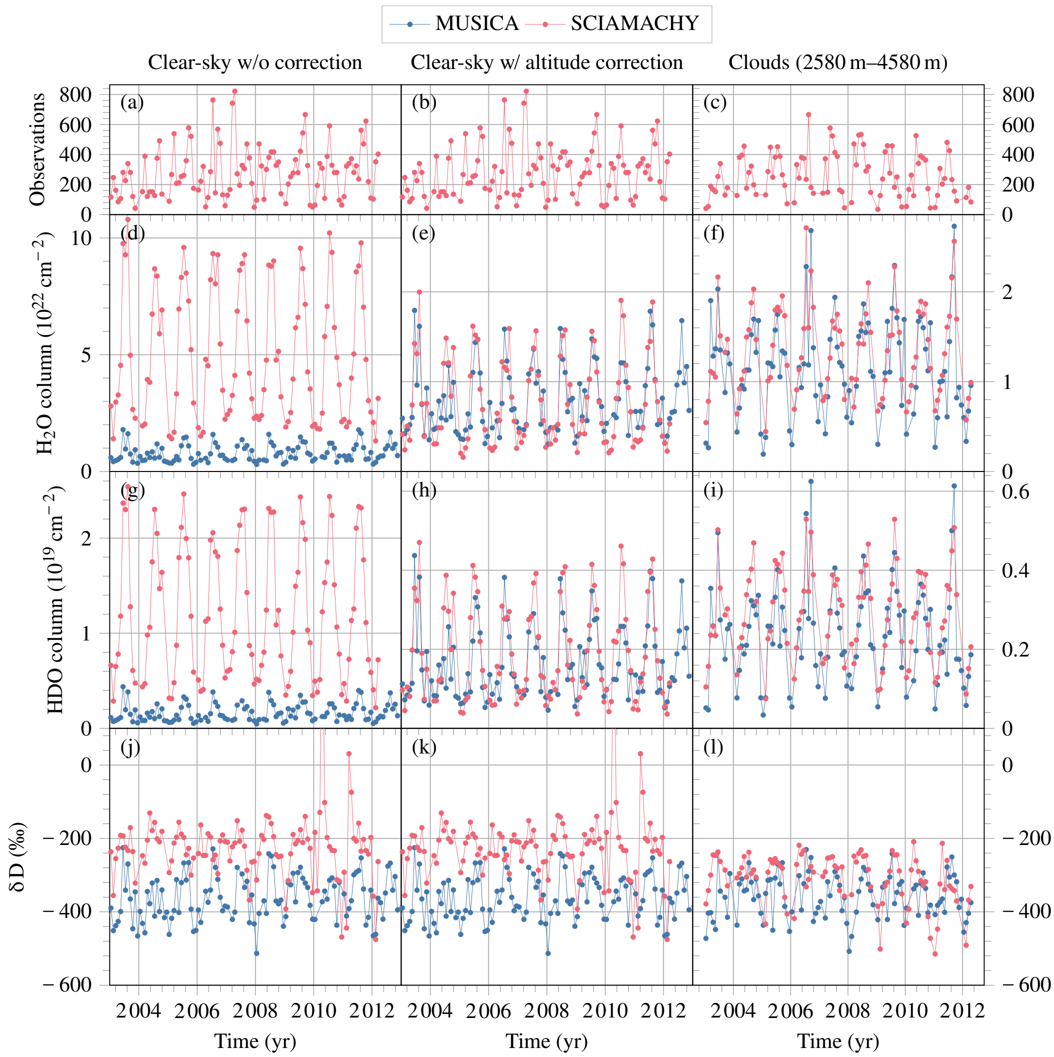

Figure 8. Time series of monthly medians similar to those shown in Fig. 3 but for scattering retrievals near the high-altitude station Jungfraujoch (3580 m a.s.l.). The left panels **(a)**, **(d)**, **(g)** and **(j)** show clear-sky measurements without altitude correction; the centre panels **(b)**, **(e)**, **(h)** and **(k)** show the same measurements with altitude correction; and the right panels **(c)**, **(f)**, **(i)** and **(l)** show observations with optically thick clouds within an altitude range 1000 m above and below the station height. Please note that in the left panels the H_2O and HDO axes are different than in the centre and right panels, as indicated by the axis ticks.

rection eliminates the large biases for H_2O and HDO for the most part: the biases are reduced by more than factors of 400 and 36 to 1.0×10^{20} molec cm^{-2} and 3.0×10^{17} molec cm^{-2}. However, for δD computed from the corrected columns, the bias remains due to the assumption in the same relative vertical distribution of both isotopologues.

Next, cloudy scenes with cloud height around the station altitude are evaluated, since for these the result for the whole column is dominated by the part above the cloud due to the measurement sensitivity. The sensitivity of the retrieved column to changes in the vertical distribution of the water vapour isotopologues is described by the column averaging kernel (e.g. Rodgers, 2004). An example of averaging kernels of clear-sky and cloudy measurements is shown in Fig. 9. A detailed discussion of the column averaging kernel is given by Borsdorff et al. (2014). In the case of an optically thick cloud (in the example at 3.5 km altitude), the retrieval is sensitive above the cloud but insensitive below the cloud, which underlines the selection criteria for cloudy-sky observations in Table 2. Furthermore, to compare MUSICA data with cloudy SCIAMACHY observations, it is important to realise that cloudy conditions usually involve a higher humidity than clear-sky conditions. The ground-based measurements are taken under the latter and so MUSICA data are first interpolated to the time of the satellite observations using ECMWF, similar to the method described by Borsdorff et al. (2016, Sect. 4.1) (compare Fig. 8e and f). A height difference between SCIAMACHY ground pixel and MUSICA station

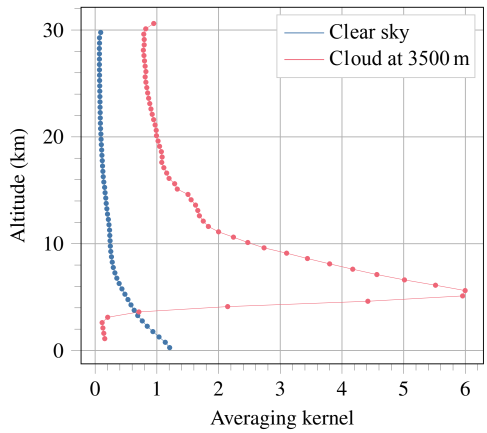

Figure 9. Example of averaging kernels for H_2O for a clear-sky measurement (blue) and a scene with optically thick clouds (red).

is corrected as described above. The right panel of Fig. 8 depicts the result. The bias in δD between SCIAMACHY and MUSICA is significantly reduced and the difference between panels k and l demonstrates the altitude dependence of δD. Only satellite measurements with similar altitude sensitivity to the ground-based observations yield good agreement.

Figure 10 presents the statistics for the scattering retrievals above the high-altitude stations Jungfraujoch and Izaña. The correlation in H_2O and HDO is generally good for all evaluations, but it is small for δD due to the noise in δD being nearly as large as its seasonality. However, the correlation increases slightly for the cloud retrieval. When looking at the bias, the behaviour already seen in the time series is confirmed. It is large for all three quantities for uncorrected clear-sky observations. The altitude correction reduces significantly the bias in H_2O and HDO, while no change occurs in δD. The latter is significantly reduced by regarding scenes with clouds at an altitude near the station height. The biases in H_2O and HDO increase slightly when going from clear-sky to cloudy scenes, but are still much lower than for the uncorrected case. This may be explained by the differences in cloud height compared to the station height accepted by the data selection.

For cloud retrievals from SCIAMACHY observations at polar latitudes the data quality is reduced. Due to the limited radiometric performance of SCIAMACHY, the retrieval of cloud properties from methane absorption feature is hampered by the low SNR for these challenging observation geometries and the dominance of water vapour absorption in the considered spectral range.

Due to these instrumental problems at polar latitudes, the non-scattering retrieval is preferred for the global SCIAMACHY data set. For the new TROPOMI instrument, however, the cloud retrieval is expected to work for all latitudes, because it has a much better signal to noise ratio and a much better radiometric calibration, and the size of the ground pixel (and thus the averaging over areas with potentially

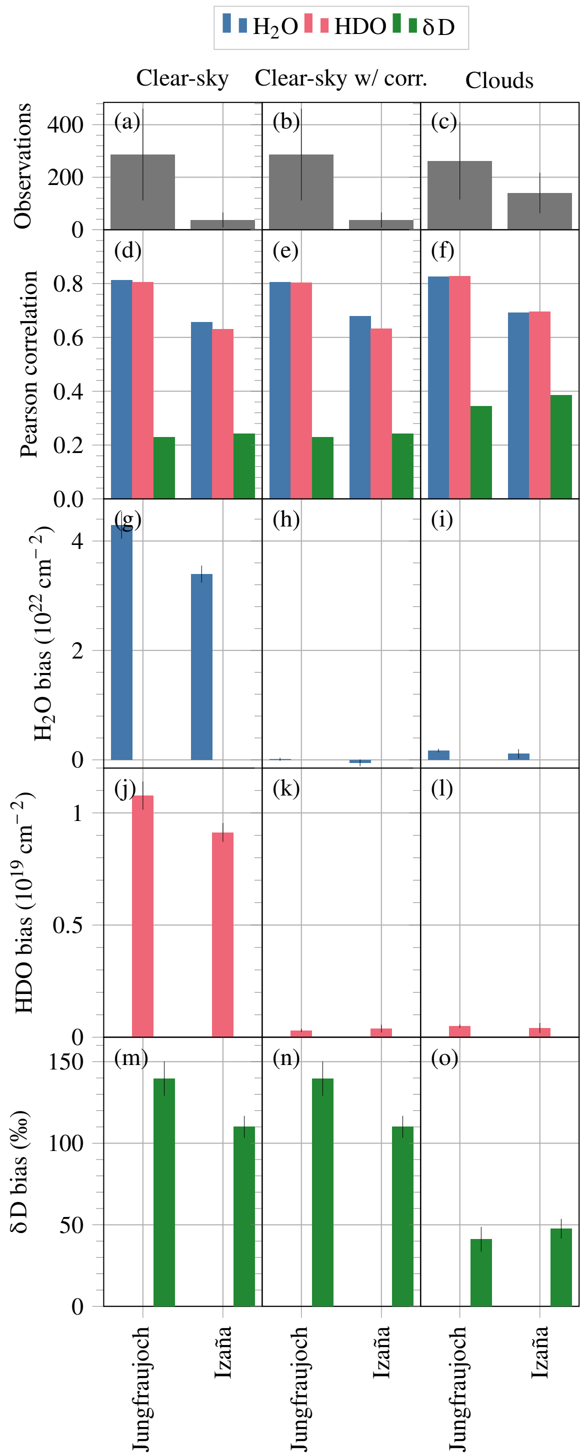

Figure 10. Like Fig. 5 but for cloud retrievals for high-altitude stations. Panels **(a)**, **(d)**, **(g)**, **(j)** and **(m)** show results for clear-sky measurements without altitude correction; **(b)**, **(e)**, **(h)**, **(k)** and **(n)** show those for clear-sky observations with altitude correction; and **(c)**, **(f)**, **(i)**, **(l)** and **(o)** show those for altitude-corrected observations with optically thick clouds within the station height plus or minus 1000 m.

varying cloud cover) is much smaller. The last point is also important, since water vapour is known to vary considerably both spatially and temporally. In this light, the current study is also preparation for future investigations with TROPOMI.

5 Summary and conclusions

In this paper a new data set of satellite observations of column densities of the water vapour isotopologues H_2O and HDO from the SCIAMACHY instrument is presented, which spans the whole mission period from January 2003 to April 2012. This is an addition of more than 4 years compared to Scheepmaker et al. (2015). To this end, the degradation of the instrument has to be mitigated by enlarging the retrieval window compared to Scheepmaker et al. (2015) and by eliminating the radiometric offset via calibration with the Sahara region as a natural target. Atmospheric light scattering is ignored in the forward simulation of the measurements. Additionally, the possibility of inferring simultaneously effective cloud parameter and the water vapour abundance is considered in a dedicated case study for measurements around high-altitude stations.

Due to the high amount of sensor noise in SCIAMACHY, averaging in time and/or space has to be adequate to obtain reasonable results. For instance, monthly medians are meaningful when averaging over a circle with 800 km radius. More spatial resolutions, such as $1^\circ \times 1^\circ$ global coverage, can be achieved when sacrificing temporal resolution by averaging over several years.

The satellite observations are validated against low-altitude ground-based FTIR measurements from the MUSICA project within the NDACC network. In general, the agreement is good. The Pearson correlation coefficient for H_2O and HDO is between 0.74 and 0.97, and the average bias is only -3.6×10^{21} for H_2O and -1.0×10^{18} molec cm^{-2} for HDO. For δD, the correlation is also good for most stations (between 0.56 and 0.79), with three exceptions where the seasonal variation is small. The bias is low except at polar stations (Eureka and Ny Ålesund). The decreased performance at high latitudes stems from imprecise measurements caused by the large amount of sensor noise in SCIAMACHY in combination with difficult measurement geometries. The average bias in δD over all stations is -8 ‰, but when excluding Eureka and Ny Ålesund it is only $+1$ ‰.

High-altitude stations (Jungfraujoch and Izaña) are treated separately in a case study with a retrieval that takes scattering into account and additionally infers cloud parameters. Since both instruments observe different altitude ranges, the bias is large for clear-sky measurements with 3.8×10^{22} molec cm^{-2} for H_2O, 1.0×10^{19} molec cm^{-2} for HDO and 125 ‰ for δD.

To correct for the altitude effect, partial columns above the station height are computed for SCIAMACHY by cutting an ECMWF water vapour profile scaled to the retrieved column. This yields good agreement between SCIAMACHY and MUSICA in H_2O and HDO, the mean biases are reduced to -2.2×10^{20} and 3.4×10^{17} molec cm^{-2}. The bias for the a posteriori δD cannot be corrected that way, however, because the profiles for H_2O and HDO have the same shape, neglecting the increasing depletion with height.

The average bias in δD is drastically reduced to 44 ‰ by considering scenes with optically thick clouds between 1000 m below and 1000 m above the station height and applying the altitude correction, since for these scenes the retrieval is sensitive predominantly above the cloud. For this approach, the results from SCIAMACHY agree well with those from MUSICA in all three quantities, H_2O, HDO and δD. The corresponding biases in H_2O and HDO are 1.4×10^{21} and 4.5×10^{17} molec cm^{-2}.

The scattering retrievals work well for low latitudes and midlatitudes, as demonstrated in the case study for high-altitude stations, but are unreliable for polar latitudes. This is caused by the limited radiometric performance of SCIAMACHY in combination with difficult observation geometries. For the newly launched TROPOMI instrument, which measures in the SWIR range with a spectral resolution similar to that of SCIAMACHY but with a much better signal to noise ratio and a much higher spatial resolution, the method is expected to work for all latitudes. Moreover, the inferred columns are expected to have a higher precision, eliminating the necessity to average over long periods of time or large areas. Thus, future investigations will concentrate on TROPOMI.

Data availability. The full-mission SCIAMACHY H_2O/HDO data set from the non-scattering retrieval described in this paper is available for download at ftp://ftp.sron.nl/pub/pub/DataProducts/SCIAMACHY_HDO/ (Schneider et al., 2017). The MUSICA data were downloaded from ftp://ftp.cpc.ncep.noaa.gov/ndacc/MUSICA/ (Barthlott et al., 2016).

Competing interests. The authors declare that they have no conflict of interest.

Acknowledgements. SCIAMACHY is a joint project between the German Space Agency DLR and the Dutch Space Agency NSO with contributions from the Belgian Space Agency. The data on the ground-based measurements have been provided by the project MUSICA, which has been funded by the European Research Council under the European Community's Seventh Framework Programme (FP7/2007–2013)/ERC grant agreement number 256961.

Edited by: Jun Wang
Reviewed by: two anonymous referees

References

Barthlott, S., Schneider, M., Hase, F., Blumenstock, T., Mengistu Tsidu, G., Grutter de la Mora, M., Strong, K., Notholt, J., Mahieu, E., Jones, N., and Smale, D.: The ground-based MUSICA dataset: Tropospheric water vapour isotopologues (H216O, H218O and HD16O) as obtained from NDACC/FTIR solar absorption spectra, https://doi.org/10.5281/zenodo.48902, 2016.

Barthlott, S., Schneider, M., Hase, F., Blumenstock, T., Kiel, M., Dubravica, D., García, O. E., Sepúlveda, E., Mengistu Tsidu, G., Takele Kenea, S., Grutter, M., Plaza-Medina, E. F., Stremme, W., Strong, K., Weaver, D., Palm, M., Warneke, T., Notholt, J., Mahieu, E., Servais, C., Jones, N., Griffith, D. W. T., Smale, D., and Robinson, J.: Tropospheric water vapour isotopologue data ($H_2^{16}O$, $H_2^{18}O$, and $HD^{16}O$) as obtained from NDACC/FTIR solar absorption spectra, Earth Syst. Sci. Data, 9, 15–29, https://doi.org/10.5194/essd-9-15-2017, 2017.

Bastrikov, V., Steen-Larsen, H. C., Masson-Delmotte, V., Gribanov, K., Cattani, O., Jouzel, J., and Zakharov, V.: Continuous measurements of atmospheric water vapour isotopes in western Siberia (Kourovka), Atmos. Meas. Tech., 7, 1763–1776, https://doi.org/10.5194/amt-7-1763-2014, 2014.

Boesch, H., Deutscher, N. M., Warneke, T., Byckling, K., Cogan, A. J., Griffith, D. W. T., Notholt, J., Parker, R. J., and Wang, Z.: HDO/H_2O ratio retrievals from GOSAT, Atmos. Meas. Tech., 6, 599–612, https://doi.org/10.5194/amt-6-599-2013, 2013.

Borsdorff, T., Hasekamp, O. P., Wassmann, A., and Landgraf, J.: Insights into Tikhonov regularization: application to trace gas column retrieval and the efficient calculation of total column averaging kernels, Atmos. Meas. Tech., 7, 523–535, https://doi.org/10.5194/amt-7-523-2014, 2014.

Borsdorff, T., Tol, P., Williams, J. E., de Laat, J., aan de Brugh, J., Nédélec, P., Aben, I., and Landgraf, J.: Carbon monoxide total columns from SCIAMACHY 2.3 µm atmospheric reflectance measurements: towards a full-mission data product (2003–2012), Atmos. Meas. Tech., 9, 227–248, https://doi.org/10.5194/amt-9-227-2016, 2016.

Borsdorff, T., aan de Brugh, J., Hu, H., Nédélec, P., Aben, I., and Landgraf, J.: Carbon monoxide column retrieval for clear-sky and cloudy atmospheres: a full-mission data set from SCIAMACHY 2.3 µm reflectance measurements, Atmos. Meas. Tech., 10, 1769–1782, https://doi.org/10.5194/amt-10-1769-2017, 2017.

Bovensmann, H., Burrows, J. P., Buchwitz, M., Frerick, J., Noël, S., Rozanov, V. V., Chance, K. V., and Goede, A. P. H.: SCIAMACHY: Mission Objectives and Measurement Modes, J. Atmos. Sci., 56, 127–150, https://doi.org/10.1175/1520-0469(1999)056<0127:SMOAMM>2.0.CO;2, 1999.

Dansgaard, W.: Stable isotopes in precipitation, Tellus, 16, 436–468, https://doi.org/10.3402/tellusa.v16i4.8993, 1964.

Dyroff, C., Fütterer, D., and Zahn, A.: Compact diode-laser spectrometer ISOWAT for highly sensitive airborne measurements of water-isotope ratios, Appl. Phys. B, 98, 537–548, https://doi.org/10.1007/s00340-009-3775-6, 2010.

Ehhalt, D. H., Rohrer, F., and Fried, A.: Vertical profiles of HDO/H_2O in the troposphere, J. Geophys. Res., 110, D13301, https://doi.org/10.1029/2004JD005569, 2005.

Frankenberg, C., Yoshimura, K., Warneke, T., Aben, I., Butz, A., Deutscher, N., Griffith, D., Hase, F., Notholt, J., Schneider, M., Schrijver, H., and Röckmann, T.: Dynamic Processes Governing Lower-Tropospheric HDO/H_2O Ratios as Observed from Space and Ground, Science, 325, 1374–1377, https://doi.org/10.1126/science.1173791, 2009.

Gloudemans, A. M. S., Schrijver, H., Kleipool, Q., van den Broek, M. M. P., Straume, A. G., Lichtenberg, G., van Hees, R. M., Aben, I., and Meirink, J. F.: The impact of SCIAMACHY near-infrared instrument calibration on CH_4 and CO total columns, Atmos. Chem. Phys., 5, 2369–2383, https://doi.org/10.5194/acp-5-2369-2005, 2005.

Harries, J. E.: Atmospheric radiation and atmospheric humidity, Q. J. Roy. Meteor. Soc., 123, 2173–2186, https://doi.org/10.1002/qj.49712354402, 1997.

Herbin, H., Hurtmans, D., Clerbaux, C., Clarisse, L., and Coheur, P.-F.: $H_2^{16}O$ and HDO measurements with IASI/MetOp, Atmos. Chem. Phys., 9, 9433–9447, https://doi.org/10.5194/acp-9-9433-2009, 2009.

Kiehl, J. T. and Trenberth, K. E.: Earth's Annual Global Mean Energy Budget, B. Am. Meteorol. Soc., 78, 197–208, https://doi.org/10.1175/1520-0477(1997)078<0197:EAGMEB>2.0.CO;2, 1997.

Landgraf, J., aan de Brugh, J., Scheepmaker, R., Borsdorff, T., Hu, H., Houweling, S., Butz, A., Aben, I., and Hasekamp, O.: Carbon monoxide total column retrievals from TROPOMI shortwave infrared measurements, Atmos. Meas. Tech., 9, 4955–4975, https://doi.org/10.5194/amt-9-4955-2016, 2016.

Predoi-Cross, A., Brawley-Tremblay, M., Brown, L. R., Devi, V. M., and Benner, D. C.: Multispectrum analysis of $^{12}CH_4$ from 4100 to 4635 cm^{-1}: II. Air-broadening coefficients (widths and shifts), J. Mol. Spectrosc., 236, 201–215, https://doi.org/10.1016/j.jms.2006.01.013, 2006.

Rinsland, C. P., Goldman, A., Devi, V. M., Fridovich, B., Snyder, D. G. S., Jones, G. D., Murcray, F. J., Murcray, D. G., Smith, M. A. H., Seals, R. K., Coffey, M. T., and Mankin, W. G.: Simultaneous stratospheric measurements of H_2O, HDO, and CH_4 from balloon-borne and aircraft infrared solar absorption spectra and tunable diode laser laboratory spectra of HDO, J. Geophys. Res., 89, 7259–7266, https://doi.org/10.1029/JD089iD05p07259, 1984.

Rodgers, C. D.: Inverse methods for atmospheric sounding: theory and practice, vol. 2, Series on atmospheric, oceanic and planetary physics, World Scientific, Singapore, 2004.

Rothman, L., Gordon, I., Barbe, A., Benner, D., Bernath, P., Birk, M., Boudon, V., Brown, L., Campargue, A., Champion, J.-P., Chance, K., Coudert, L., Dana, V., Devi, V., Fally, S., Flaud, J.-M., Gamache, R., Goldman, A., Jacquemart, D., Kleiner, I., Lacome, N., Lafferty, W., Mandin, J.-Y., Massie, S., Mikhailenko, S., Miller, C., Moazzen-Ahmadi, N., Naumenko, O., Nikitin, A., Orphal, J., Perevalov, V., Perrin, A., Predoi-Cross, A., Rinsland, C., Rotger, M., Šimečková, M., Smith, M., Sung, K., Tashkun, S., Tennyson, J., Toth, R., Vandaele, A., and Auwera, J. V.: The HITRAN 2008 molecular spectroscopic database, J. Quant. Spectrosc. Ra., 110, 533–572, https://doi.org/10.1016/j.jqsrt.2009.02.013, 2009.

Scheepmaker, R. A., Frankenberg, C., Galli, A., Butz, A., Schrijver, H., Deutscher, N. M., Wunch, D., Warneke, T., Fally, S., and Aben, I.: Improved water vapour spectroscopy in the 4174–4300 cm^{-1} region and its impact on SCIAMACHY

HDO/H_2O measurements, Atmos. Meas. Tech., 6, 879–894, https://doi.org/10.5194/amt-6-879-2013, 2013.

Scheepmaker, R. A., Frankenberg, C., Deutscher, N. M., Schneider, M., Barthlott, S., Blumenstock, T., Garcia, O. E., Hase, F., Jones, N., Mahieu, E., Notholt, J., Velazco, V., Landgraf, J., and Aben, I.: Validation of SCIAMACHY HDO/H_2O measurements using the TCCON and NDACC-MUSICA networks, Atmos. Meas. Tech., 8, 1799–1818, https://doi.org/10.5194/amt-8-1799-2015, 2015.

Scheepmaker, R. A., aan de Brugh, J., Hu, H., Borsdorff, T., Frankenberg, C., Risi, C., Hasekamp, O., Aben, I., and Landgraf, J.: HDO and H_2O total column retrievals from TROPOMI shortwave infrared measurements, Atmos. Meas. Tech., 9, 3921–3937, https://doi.org/10.5194/amt-9-3921-2016, 2016.

Schneider, A., Borsdorff, T., aan de Brugh, J., Hu, H., and Landgraf, J.: A full-mission data set of H_2O and HDO columns from SCIAMACHY 2.3 µm reflectance measurements, available at: ftp://ftp.sron.nl/pub/pub/DataProducts/SCIAMACHY_HDO/ (last access: 6 June 2018), 2017.

Schneider, M., Hase, F., and Blumenstock, T.: Water vapour profiles by ground-based FTIR spectroscopy: study for an optimised retrieval and its validation, Atmos. Chem. Phys., 6, 811–830, https://doi.org/10.5194/acp-6-811-2006, 2006.

Schneider, M., Barthlott, S., Hase, F., González, Y., Yoshimura, K., García, O. E., Sepúlveda, E., Gomez-Pelaez, A., Gisi, M., Kohlhepp, R., Dohe, S., Blumenstock, T., Wiegele, A., Christner, E., Strong, K., Weaver, D., Palm, M., Deutscher, N. M., Warneke, T., Notholt, J., Lejeune, B., Demoulin, P., Jones, N., Griffith, D. W. T., Smale, D., and Robinson, J.: Ground-based remote sensing of tropospheric water vapour isotopologues within the project MUSICA, Atmos. Meas. Tech., 5, 3007–3027, https://doi.org/10.5194/amt-5-3007-2012, 2012.

Schneider, M., Wiegele, A., Barthlott, S., González, Y., Christner, E., Dyroff, C., García, O. E., Hase, F., Blumenstock, T., Sepúlveda, E., Mengistu Tsidu, G., Takele Kenea, S., Rodríguez, S., and Andrey, J.: Accomplishments of the MUSICA project to provide accurate, long-term, global and high-resolution observations of tropospheric $\{H_2O,\delta D\}$ pairs – a review, Atmos. Meas. Tech., 9, 2845–2875, https://doi.org/10.5194/amt-9-2845-2016, 2016.

Steinwagner, J., Milz, M., von Clarmann, T., Glatthor, N., Grabowski, U., Höpfner, M., Stiller, G. P., and Röckmann, T.: HDO measurements with MIPAS, Atmos. Chem. Phys., 7, 2601–2615, https://doi.org/10.5194/acp-7-2601-2007, 2007.

Stevens, B. and Bony, S.: What Are Climate Models Missing?, Science, 340, 1053–1054, https://doi.org/10.1126/science.1237554, 2013.

Stowasser, M., Oelhaf, H., Wetzel, G., Friedl-Vallon, F., Maucher, G., Seefeldner, M., Trieschmann, O., v. Clarmann, T., and Fischer, H.: Simultaneous measurements of HDO, H_2O, and CH_4 with MIPAS-B: Hydrogen budget and indication of dehydration inside the polar vortex, J. Geophys. Res., 104, 19213–19225, https://doi.org/10.1029/1999JD900239, 1999.

Veefkind, J., Aben, I., McMullan, K., Förster, H., de Vries, J., Otter, G., Claas, J., Eskes, H., de Haan, J., Kleipool, Q., van Weele, M., Hasekamp, O., Hoogeveen, R., Landgraf, J., Snel, R., Tol, P., Ingmann, P., Voors, R., Kruizinga, B., Vink, R., Visser, H., and Levelt, P.: TROPOMI on the ESA Sentinel-5 Precursor: A GMES mission for global observations of the atmospheric composition for climate, air quality and ozone layer applications, Remote Sens. Environ., 120, 70–83, https://doi.org/10.1016/j.rse.2011.09.027, 2012.

Wen, X.-F., Zhang, S.-C., Sun, X.-M., Yu, G.-R., and Lee, X.: Water vapor and precipitation isotope ratios in Beijing, China, J. Geophys. Res., 115, D01103, https://doi.org/10.1029/2009JD012408, 2010.

Worden, J., Bowman, K., Noone, D., Beer, R., Clough, S., Eldering, A., Fisher, B., Goldman, A., Gunson, M., Herman, R., Kulawik, S. S., Lampel, M., Luo, M., Osterman, G., Rinsland, C., Rodgers, C., Sander, S., Shephard, M., and Worden, H.: Tropospheric Emission Spectrometer observations of the tropospheric HDO/H_2O ratio: Estimation approach and characterization, J. Geophys. Res., 111, D16309, https://doi.org/10.1029/2005JD006606, 2006.

Zakharov, V. I., Imasu, R., Gribanov, K. G., Hoffmann, G., and Jouzel, J.: Latitudinal distribution of the deuterium to hydrogen ratio in the atmospheric water vapor retrieved from IMG/ADEOS data, Geophys. Res. Lett., 31, L12104, https://doi.org/10.1029/2004GL019433, 2004.